J. Membrane Biol. 152, 245–252 (1996)

The Journal of
Membrane
Biology

Activity and Stoichiometry of Na^+:HCO_3^- Cotransport in Immortalized Renal Proximal Tubule Cells

E. Gross, U. Hopfer
Department of Physiology and Biophysics, Case Western Reserve University, 10900 Euclid Ave., Cleveland, OH, 44106-4970

Received: 19 January 1996/Revised: 24 April 1996

Abstract. The proximal tubule Na^+-HCO_3^- cotransporter is located in the basolateral plasma membrane and moves Na^+, HCO_3^-, and net negative charge together out of the cell. The presence of charge transport implies that at least two HCO_3^- anions are transported for each Na^+ cation. The actual ratio is of physiological interest because it determines direction of net transport at a given membrane potential. To determine this ratio, a thermodynamic approach was employed that depends on measuring charge flux through the cotransporter under defined ion and electrical gradients across the basolateral plasma membrane. Cells from an immortalized rat proximal tubule line were grown as confluent monolayer on porous substrate and their luminal plasma membrane was permeabilized with amphotericin B. The electrical properties of these monolayers were measured in a Ussing chamber, and ion flux through the cotransporter was achieved by applying Na^+ or HCO_3^- concentration gradients across the basolateral plasma membrane. Charge flux through the cotransporter was identified as difference current due to the reversible inhibitor dinitrostilbene disulfonate. The cotransporter activity was Cl^- independent; its conductance ranged between 0.12 and 0.23 mS/cm^2 and was voltage independent between −60 and +40 mV. Reversal potentials obtained from current-voltage relations in the presence of Na^+ gradients were fitted to the thermodynamic equivalent of the Nernst equation for coupled ion transport. The fit yielded a cotransport ratio of $3HCO_3^-$:$1Na^+$.

Key words: Amphotericin B — Dinitro-stilbene disulfonic acid — Na^+-HCO_3^- cotransporter — Proximal tubule — Rat, transport ratio — Ussing chamber

Correspondence to: U. Hopfer

Introduction

The proximal convoluted tubule in higher vertebrates is responsible for reabsorption of filtered bicarbonate (HCO_3^-). The epithelial cells achieve this reabsorption by secreting protons into the lumen and an equal number of base equivalents across the basolateral plasma membrane into the peritubular space. A Na^+-HCO_3^- cotransporter has been identified in the basolateral plasma membrane of several species as responsible transporter for extrusion of base (Boron & Boulpaep, 1983; Burckhardt, Sato & Fromter, 1984; Yoshitomi & Fromter, 1984; Alpern, 1985; Biagi, 1985; Jentsch et al., 1985, 1986; Sasaki, Shiigai & Takeuchi, 1985; Yoshitomi, Burckhardt & Fromter, 1985; Akiba et al., 1986; Alpern & Chambers, 1986; Biagi & Sohtell, 1986; Lopes et al., 1987; Soleimani, Grassl & Aronson, 1987). The cotransporter has been found to be electrogenic and linked to a net flux of negative charge (Boron & Boulpaep, 1983; Biagi, 1985; Jentsch et al., 1985; Sasaki et al., 1985; Yoshitomi et al., 1985; Biagi & Sohtell, 1986; Lopes et al., 1987). This property indicates that the stoichiometry of the process involves more than one HCO_3^- cotransported per each Na^+. Knowledge of the precise stoichiometry is important for predicting direction of net transport. The larger the stoichiometry, and hence the larger the net negative charge movement per transport cycle, the more effective is the membrane potential as driving force to move HCO_3^- out of the cell. The best estimates are a ratio of 3:1 for HCO_3^-:Na^+ based on rates of concentration changes in rat proximal tubule in vivo (Yoshitomi et al., 1985) and on driving forces necessary to prevent solute flux through the cotransporter in rabbit basolateral plasma membrane vesicle (Soleimani et al., 1987). Both estimates depend on a number of assumptions or parameters that are difficult to measure with certainty, such as cellular buffer capacity or formation of ideal diffusion potentials.

Table 1. Composition of solutions (concentrations in mM)

	Normal K	K-free Low Cl^-		Cl^- free				
Solution	1	2	3	4	5	6	7	8
Na-Gluc	40	40	10	40	40	10	20	60
NMDG	100	104.7	134.7	104.7	104.7	134.7	124.7	84.7
HCO_3^-*	10	10	10	10	2	10	10	10
KCl	4.7	0	0	0	0	0	0	0
$MgCl_2$	1.13	1.13	1.13	0	0	0	0	0
$CaCl_2$	2.25	2.25	2.25	0	0	0	0	0
$Ca\text{-}Gluc_2$	0	0	0	2.25	2.25	2.25	2.25	2.25
$Mg\text{-}Gluc_2$	0	0	0	1.13	1.13	1.13	1.13	1.13
HEPES	20	20	20	20	20	20	20	20
D-Glucose	25	25	25	25	25	25	25	25
pH	7.0	7.0	7.0	7.0	6.4	7.0	7.0	7.0

* $[HCO_3^-]$ was calculated according to the relation: $[HCO_3^-] = 3 \cdot 10^{-5} \cdot 760 \cdot f \cdot 10^{(pH-6.1)}$ where f is the CO_2 partial pressure.

All solutions were ''preincubated'' in the voltage-clamp setup incubator at 37°C and 5% CO_2 for 2 hr before the beginning of the experiment.

All solutions were supplemented with 0.1% BSA.

Because of the importance of the cotransporter stoichiometry for overall HCO_3^- absorption in the proximal tubule and uncertainties in the limited number of studies so far, we have reinvestigated this question in a new cell model, namely a recently immortalized cell line from rat renal proximal tubule. The cells form relatively high resistance monolayers so that electrophysiological measurements are feasible. To determine the stoichiometry, the current through the cotransporter was isolated as difference current due to the inhibitor dinitro-stilbene-disulfonate (DNDS) and the reversal potential determined in the presence of a Na^+ gradient. Information on the reversal potential and the Na^+ gradient can be used to calculate the stoichiometry based on thermodynamic considerations.

Materials and Methods

Cell Culture

Experiments were carried with the rat proximal tubular cell line SKPT-0193 Cl.2 (Woost et al., 1996). The line was derived from microdissected primary cultures of the S1 region of the proximal tubule. Cells were immortalized by infection with a retroviral vector coding for SV40 large T antigen. Passages 80 to 100 were used for the reported experiments. Cells were grown on collagen-coated (20% Ethicon in 60% ethanol) Millicell-CM filters (area = 0.6 cm^2) in a 1:1 mixture of Dulbecco's Modified Essential Medium and Ham's F12, supplemented with 15 mM HEPES, 1.2 mg/ml $NaHCO_3$, 5 μg/ml insulin, 5 μg/ml transferrin, 10 ng/ml Epithelial Growth Factor, 4 μ g/ml dexamethasone, and 10% fetal bovine serum. Usually, about 3×10^5 cells were seeded and grown to confluence in five days. Light microscopy showed ''cobble stone'' appearance that is typical for epithelial cells. No piling of cells was observed.

Electrophysiology

Filters were mounted horizontally in a Ussing-type chamber (Analytical Bioinstrumentation, Cleveland, OH) equipped with a pair of voltage and a pair of current electrodes. Electrophysiological measurements were made with a voltage-clamp module (Model 558-C-5, Bioengineering, University of Iowa, IA). The data were recorded on a strip-chart recorder and in parallel through an A/D converter on a microcomputer. The Ussing chamber and all solutions were maintained in a heated incubator to control the partial pressure of CO_2 and temperature. Experiments were carried out at 37°C and at 5% CO_2. CO_2 pressure was continuously monitored with a CO_2 monitor (Puritan-Bennett, Los Angeles, CA). The filter in the Ussing chamber was perfused with modified Ringer solutions as explained in the text. The composition of different solutions is given in Table 1.

Materials

Amphotericin B, bovine serum albumin, HEPES, D-glucose, N-methyl-D-glucamine (NMDG), gluconic acid, and all salts were purchased from Sigma Chemical (St. Louis, MO). Dinitro-stilbene-disulfonate (DNDS) was obtained from Pfaltz & Bauer, (Waterbury, CT).

Results

Properties of a Proximal Tubular Cell Line

The cell line for this study was derived from microdissected proximal tubule S1 segments of rats. This segment is known to contain considerable Na^+-HCO_3^- cotransporter activity. The cells formed confluent monolayers on the filters. One of the interesting characteristics was the relative low monolayer conductance of about 1 mS/cm^2 due to poor ion permeability of tight junctions. This low baseline conductance allowed the detection of

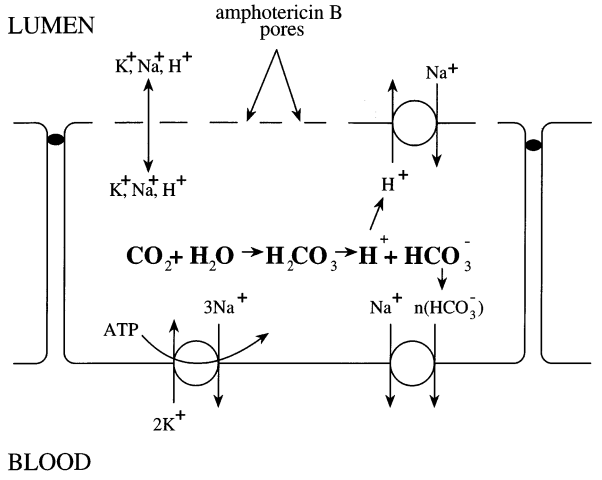

Fig. 1. Schematic presentation of the premises on which experiments were based. The Na^+-HCO_3^- cotransporter and Na^+,K^+ ATPase transport ($n - 1$) net negative and one positive charge, respectively. The Na^+/H^+ exchanger is electrically silent. Luminal application of amphotericin B ''removes'' functionally the luminal membrane for electrical measurements.

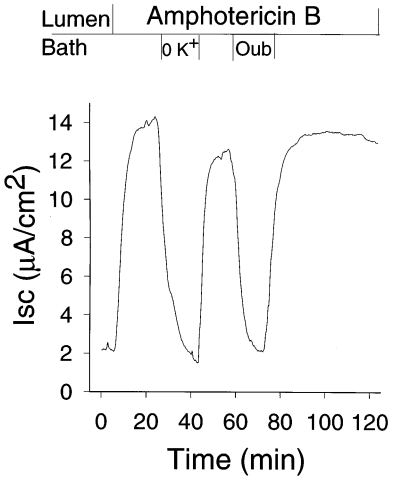

Fig. 2. Short-circuit current (I_{sc}) of a luminally permeabilized monolayer. Cells were initially perfused with normal-K^+ Ringer (solution #1). The increased I_{sc} following luminal application of amphotericin B reflects the activity of the Na^+, K^+ ATPase. Inhibition of the enzyme upon removal of K^+ (OK^+) (perfusion with K^+-free Ringer (solution #2)) or upon basolateral application of 1 mM ouabain (Oub) results in a decrease in I_{sc}.

electrical signals from cellular transporters without too much ''background'' conductance from the paracellular pathway for ion flow.

Experimental Strategy

Figure 1 illustrates the transporters that are thought to be involved in Na^+ HCO_3^- reabsorption in the proximal tubule. The transporters associated with electrical charge movement are located in the basolateral membrane. These include the Na^+,K^+-ATPase (the pump), the Na^+-HCO_3^- cotransporter, and K^+ channels. To reveal these electrogenic processes to external electrodes, it was necessary to remove the electrical resistance of the luminal plasma membrane. The polyene ionophore amphotericin B has been used to specifically achieve this aim in monolayers of epithelial cells (Kirk & Dawson, 1983). Amphotericin B renders the membrane permeable to small monovalent ions (Na^+, K^+, Cl^-), but not to those with higher valences, such as Ca^{2+}, and stays restricted for several hours to the plasma membrane to which it was added. This property is a result of a requirement for cholesterol in the membrane, the relatively high cholesterol content of the plasma membrane, and the relatively low content of intracellular membranes.

With permeabilization of the luminal membrane to monovalent ions, the Na^+,K^+-ATPase turnover can be measured by its ability to generate a current in symmetrical solutions, i.e., in the absence of any electrical potential, ion concentration gradients, or osmotic or hydrostatic pressure differences. In other words, the short-circuit current with identical solutions on both sides quantitatively measures pump turnover. To identify currents associated with Na^+-HCO_3^- cotransporter activity, the electrical current in response to appropriate ionic gradients or cotransporter-specific conductance needs to be measured. The cotransporter is known to be inhibited by stilbene disulfonates. Therefore, the general approach for sorting out Na^+-HCO_3^- transport was to permeabilize monolayers on the luminal side with amphotericin B and to measure either current generated by Na^+ or HCO_3^- gradients or conductance that could be inhibited by the stilbene disulfonate DNDS. DNDS is a reversible inhibitor of the Na^+-HCO_3^- cotransporter which allows meaningful control measurements after wash-out of the drug.

Permeabilization of the Luminal Plasma Membrane by Amphotericin B

Figure 2 shows the effect of luminal application of amphotericin B. The permeabilization process can be conveniently followed by the short-circuit current (I_{sc}). The initial current is a result of a redistribution of ions after permeabilization as well as ion flux generated by pumps in the basolateral plasma membrane in response to ion influx across the luminal plasma membrane. By definition, the change in steady-state current after permeabilization is due to cellular ion pumps, either directly or indirectly. The concentration of amphotericin B used in the experiment in Fig. 2 was 40 μM, which is optimal in that it is the lowest concentration that gave a maximal change in steady-state current. This value had been established in preliminary experiments.

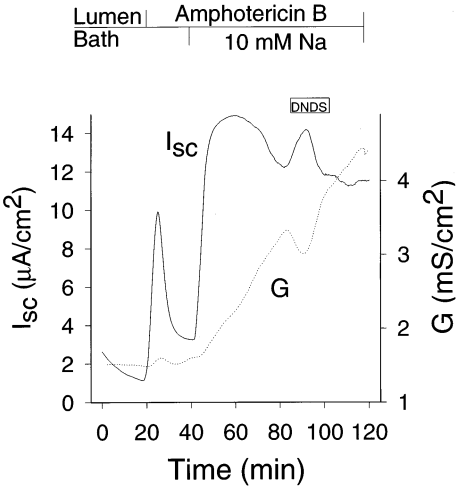

Fig. 3. Activation of Na^+-HCO_3^- cotransport by a Na^+ gradient. Current and conductance traces were measured in a Ussing chamber. Luminal and basal compartments were initially perfused with a K^+-free, 40 mM Na^+ solution (solution #2). Permeabilization with amphotericin B produced only a transient peak in current because Na,K-ATPase was inhibited by the lack of K^+. Subsequently, a Na^+-gradient (luminal 40 mM to basal 10 mM) was established by decreasing basal compartment Na^+ to 10 mM (solution #3). The Na^+ gradient produced a Na^+ flux and large I_{sc} that includes contributions by the cotransporter. Subsequent basal application of the cotransporter inhibitor DNDS revealed a DNDS-sensitive current and conductance. The DNDS-sensitive component is observable even on the background of a Cl^- conductance that is increasing with time (compare the time-dependence of conductance in the presence of Cl^- in Fig. 3 with the lack of a time-dependent component in Cl^--free medium in Fig. 4).

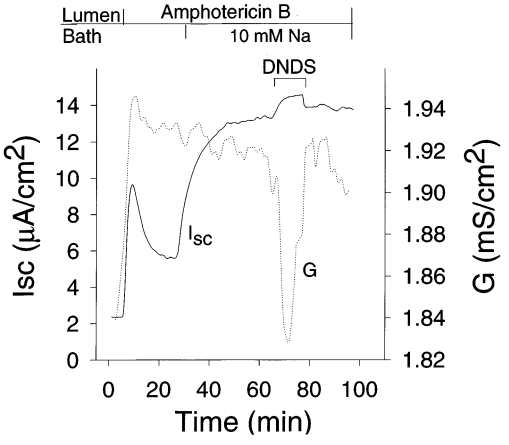

Fig. 4. Activation of Na^+-HCO_3^- cotransporter by a Na^+ gradient in Cl^--free solution. Current and conductance traces were measured in a Ussing chamber. This experiment is similar to that in Fig. 3, except for the lack of Cl^-. Luminal and basal compartments were initially perfused with a K^+- and Cl^--free, 40 mM Na^+ solution (solution #4). Activation of the Na^+-HCO_3^- cotransporter was achieved by establishing a Na^+-gradient (luminal 40 mM to basal 10 mM) with Cl^--free solution (solution #6) on the basal side. The addition of 1 mM DNDS to the basal compartment reveals a DNDS-sensitive current and conductance even in the absence of Cl^-.

After permeabilization, I_{sc} (equivalent to cation flux from luminal to basal compartment) increased steeply and then leveled off. Based on several criteria, the steady-state current represents largely Na^+, K^+-ATPase turnover: (i) The current could be reversibly inhibited by replacement of K^+ (solution #1, Table 1) with $NMDG^+$ (solution #2) in both luminal and basal solution (Fig. 2). (ii) It could be reversibly inhibited by 1 mM ouabain added to the basal solution (Fig. 2). (iii) The current depended on the presence of Na^+ in the perfusion solutions (*data not shown*). The amphotericin B permeabilization did not substantially increase the total monolayer conductance (*data not shown*). These results demonstrate that the amphotericin B-treated monolayers retained a substantial degree of cellular and monolayer integrity, even though, the luminal membrane became permeable to monovalent ions and thus electrically conductive. Others, have shown that under these conditions, the intracellular monovalent ion composition equilibrates with that of the luminal solution (Kirk & Dawson, 1983).

Na^+-HCO_3^- Transporter Activity

Flux through the Na^+-HCO_3^- cotransporter can be driven by Na^+ and/or HCO_3^- gradients as well as by an electrical potential as long as the coupling ratio of Na^+:HCO_3^- is different from 1. To measure ion gradient-driven cotransporter turnover, Na^+ or HCO_3^- gradients were established. The I_{sc} generated by these gradients, however, has contributions from all conductance pathways in the monolayer, in particular the paracellular pathway with the tight junction and the lateral intercellular space. To identify the Na^+-HCO_3^- cotransporter activity, the difference current due to the presence of 1 mM DNDS in the basolateral solution was measured.

An experiment demonstrating the cotransporter activity driven by a Na^+ gradient is shown in Fig. 3. The experiment shows the initial low I_{sc} generated by the monolayer when perfused with a modified Ringer solution (solution #2) with 40 mM Na^+, no K^+, and only 4.8 mM Cl^- (with replacement by gluconate). Luminal permeabilization generated a fast transient because Na^+,K^+-ATPase activity is not sustained when K^+ is replaced by $NMDG^+$. The imposition of a Na^+ gradient by lowering the Na^+ concentration in the basal compartment (replacement with solution #3) generated an I_{sc} of about 14 $\mu A/cm^2$ as well as a gradual increase in conductance (G) measured with small current pulses. Contributions to the current and to the conductance by the cotransporter could be demonstrated by the effects of 1 mM DNDS in the basal solution. The conductance decreased about 0.25 mS/cm^2 while the current (lumen $\rightarrow$ basal compartment) increased by about 2 $\mu A/cm^2$ as expected for inhibition of a luminal-to-basal anion (negative) current.

A Na^+-dependent Cl^--HCO_3^- exchanger has been described in a variety of mammalian cells (Boyarsky et

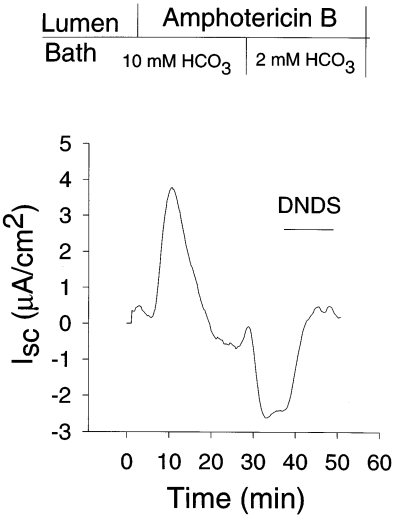

Fig. 5. Activation of Na^+-HCO_3^- cotransport by a HCO_3^- gradient. The current trace was measured in a Ussing chamber. Luminal and basal compartments were initially perfused with a K^+- and Cl^--free, 40 mM Na^+ solution containing 10 mM HCO_3^- (solution #4). The cotransporter was activated by establishing a HCO_3^--gradient (luminal 10 mM HCO_3^- to basal 2 mM) by switching to solution #5 on the basal side. The latter solution has a pH of 6.4 and HCO_3^- of 2 mM at 5% CO_2. The resulting negative current returns to baseline levels upon basal application of 1 mM DNDS as expected for flux through the cotransporter.

al., 1988; L'Allemain, Paris, & Poussegur, 1985; Rothenberg et al., 1983). We, thus, wanted to determine whether the proximal tubule cotransporter is Cl^--dependent. To this aim we repeated the procedure described in Fig. 3 for the activation of the cotransporter after Cl^- was completely eliminated from the medium (solutions #4 and #5, with Cl^- replaced by gluconate). A representative result of such an experiment is depicted in Fig. 4. Elimination of Cl^- from the bathing media did not eliminate DNDS-sensitive current and conductance; in agreement with the presence of Cl^--independent cotransporter. Further experiments were carried out in the absence of Cl^-.

Figure 5 shows the effect of lowering basolateral (bl) $[HCO_3^-]_{bl}$ from 10 mM to 2 mM by lowering the pH from 7.0 to 6.4, at constant CO_2 pressure (P_{CO_2}), (replacing solution #4 on the basolateral side with solution #5). This manipulation resulted in a 2.1 μA/cm² decrease in I_{sc}. 1 mM DNDS added to the basal solution reversed the effect (Fig. 5). In control experiments in the absence of Na^+ (Na^+ replaced with $NMDG^+$ on both the luminal and basolateral buffers), lowering $[HCO_3^-]_{bl}$ had no effect on I_{sc} (*not shown*). Table 2 summarizes the effects of lowering peritubular Na^+ and HCO_3^- on the DNDS-sensitive I_{sc}. It should be noted that in order to lower $[HCO_3^-]_{bl}$, from 10 mM to 2 mM, the pH of the basal solution had to be reduced from 7.0 to 6.4. This may add a complicating factor, as it generates a pH gradient across the basolateral membrane, but has the advantage of avoiding CO_2 gradient that would be difficult to maintain across a membrane and in the intracellular space due to the high membrane permeability of CO_2.

Table 2. Response of DNDS-sensitive currents (ΔI) to imposed ionic gradients

Ratio	ΔI (μA/cm²)[a]	*n*
$[Na^+]$i/o = 40/10[b]	1.8 ± 0.3	6
$[HCO_3^-]$i/o = 10/2[c]	2.1 ± 0.6	3

[a] Mean ± SD, *n* is the number of monolayers.
[b] (luminal solution − #2/bath solution − #3)
[c] (luminal solution − #4/bath solution − #5)

One of the complications of permeabilized monolayers is that the conductance can increase with time. This increase can interfere with the reliability of data on difference currents that depend on sequential application and removal of an inhibitor. Such an increase in conductance with time is apparent in Fig. 3 but not in Fig. 4. Because the major difference in condition between the two experiments is the absence of Cl^- from Fig. 4, the results indicate that the permeabilized rat cell monolayers develops a Cl^- conductance with time.

The Stoichiometry of the Na^+-HCO_3^- Cotransporter

The cotransport of Na^+ and HCO_3^- across the basolateral membrane can be described by:

$$Na_i + nHCO_{3i}^- \leftrightarrow Na_o^+ + nHCO_{3o}^- \quad (1)$$

where the subscripts *i* and *o* stand for inside and outside compartments, respectively. The cotransport stoichiometry of the Na^+-HCO_3^- cotransporter can be determined by finding Na^+ and/or HCO_3^- concentration gradients and membrane potentials at which no flux through the cotransporter occurs because electrical and chemical driving force balance each other. The cotransporter reaction (Eq. 1) is at equilibrium and no net flux occurs when:

$$\Delta\mu_{Na}^{i\text{-}o} = n\Delta\mu_{HCO_3}^{o\text{-}i} \quad (2)$$

where $\Delta\mu_{Na}^{i\text{-}o}$ is the in-to-out electrochemical potential difference for Na^+, $\Delta\mu_{HCO_3}^{o\text{-}i}$ is the out-to-in electrochemical potential difference for HCO_3^-, and *n* is the number of HCO_3^- anions cotransported with each Na^+ cation. Expressing the electrochemical potential differences in terms of the relevant ion concentrations and the membrane potential, V_m, yields:

$$\frac{[Na^+]_i}{[Na^+]_o} exp\frac{FV_m}{RT} = \left\{\frac{[HCO_3^-]_o}{[HCO_3^-]_i} exp\frac{FV_m}{RT}\right\}^n \quad (3)$$

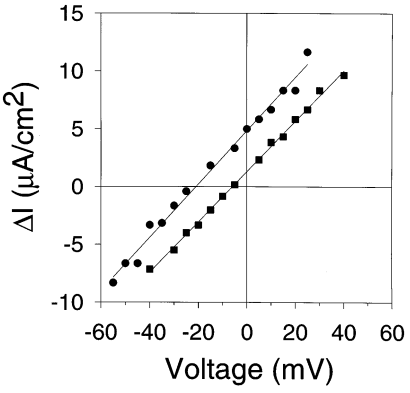

Fig. 6. Current-voltage relation for the cotransporter in luminally permeabilized monolayers. ΔI is the DNDS-sensitive current. The potential of the basal compartment is taken as zero. Luminal and basal compartments were initially perfused with 10 mM Na^+, Cl^--free solution (solution #6). $[Na^+]_{bl}$ was elevated from 10 mM to either 20 mM (solution #7) (squares) or 60 mM (solution #8) (circles), while $[Na^+]_{ap}$ was kept at 10 mM. A straight line was fitted to the data of which the slope is equal to the conductance of the cotransporter. The slopes are 0.22 (circles) and 0.23 mS/cm^2 (squares). The reversal potential is −8.5 mV (squares) and −25 mV (circles). Each experiment was repeated three times. Data represent average values.

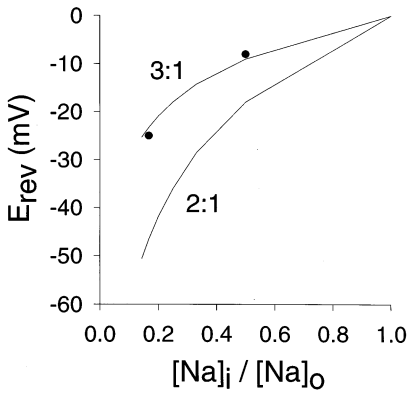

Fig. 7. Plots of E_{rev} vs. $[Na^+]_i/[Na^+]_o$ for n = 2 and n = 3. The plots were generated using Eq. 4 with $[HCO_3^-]_i/[HCO_3^-]_o = 1$. Also depicted are the measured E_{rev} values for two $[Na^+]_i/[Na^+]_o$ ratios, calculated from Fig. 6. These experimental data indicate a $3HCO_3^-$: $1Na^+$ cotransport ratio.

where F, R and T have their usual meaning and the subscripted square brackets i and o represent the concentrations of the indicated ions inside and outside the cell. The membrane potential (V_m) at which no flux (current) occurs is called reversal potential (E_{rev}) and can be experimentally determined from the current-voltage relationship. E_{rev} can be used to evaluate the actual HCO_3^- to Na^+ transport ratio, n, according to:

$$E_{rev} = \frac{RT}{F(n-1)} \ln \frac{[Na^+]_i\,[HCO_3^-]_i^n}{[Na^+]_o\,[HCO_3^-]_o^n} \qquad (4)$$

Eq. 4 suggests that E_{rev} depends logarithmically on the intra- to extracellular ratio of Na^+ and of HCO_3^- concentrations; as well as on the cotransport ratio.

The Reversal Potential

E_{rev} for the Na^+-HCO_3^- cotransporter was determined from the current-voltage relation. Figure 6 shows ΔI *vs.* V for luminally permeabilized monolayers, where ΔI is the difference in current in absence and presence of 1 mM DNDS and V is the transepithelial voltage. As was shown by others (Kirk & Dawson, 1983), the complete voltage drop is across the basolateral membrane when the luminal membrane is permeabilized with amphotericin B. Initially, cells were perfused with 10 mM Na^+, 10 mM HCO_3^- (pH 7.0) modified Ringer solution (solution #6). Following luminal membrane permeabilization with amphotericin B (40 μM) and stabilization of I_{sc}, $[Na^+]_{bl}$ was elevated to either 20 mM (solution #7) or 60 mM (solution #8), while $[HCO_3^-]$, and the partial pressure of CO_2, on both sides remained unchanged. The voltage across the monolayer was then stepped to various values, between −60 and +40 mV, and the current was recorded after a 5-sec delay to avoid transients. This procedure was repeated with 1 mM DNDS added to the basal compartment. It should be noted that in these experiments the $[Na^+]$ gradient drives the Na^+-HCO_3^- cotransporter in the ''reverse'' direction at zero membrane potential.

As shown in Fig. 6, the reversal potential (E_{rev}) for the cotransporter (V at $I = 0$) depends on the intracellular to extracellular sodium concentration ratio: it is −8.5 mV and −25 mV for $[Na^+]_i/[Na^+]_o$ ratios of 0.5 and 0.167, respectively. Note that at zero potential ($V = 0$), the cotransporter current (I_{sc}) is positive for both ratios. This is expected since, in this experiment, $[Na^+]_{bl}$ was set higher than $[Na^+]_i$ and thus the cotransporter was operating in reverse direction at zero membrane potential.

In Fig. 7, E_{rev} is plotted as a function of $[Na^+]_i/[Na^+]_o$ according to Eq. 4, whereby cotransport ratios (n) of 3 and 2 where assumed. The measured E_{rev} data from Fig. 6 are located very close to the curve which corresponds to a cotransport ratio of 3 HCO_3^-:1 Na^+.

Discussion

The findings of the present study strongly support the existence of an electrogenic Na^+-HCO_3^- cotransporter in the basolateral membrane of a recently generated proximal tubule cell line. The electrogenic cotransporter model, illustrated in Fig. 1 predicts that setting $[Na^+]_{bl} < [Na^+]_i$ at constant P_{CO_2}, should drive the cotransporter ''forward'' and thus result with the exit of a net negative charge and hence negative current. Our data clearly show that setting $[Na^+]_{bl} < [Na^+]_i$ produces the predicted

Table 3. Cl^--dependent and Cl^--independent DNDS-sensitive conductance (all solutions containing 10 mM HCO_3^-)

Solution	$[Cl^-]$ (mM)	G (mS/cm^2)*	*n*
#2	6.8	0.30	2
#4	0	0.12	2

* Mean, *n* is the number of monolayers.

effect (Figs. 3 and 4). Exit of a net negative charge would depolarize the inside negative, membrane potential as it would decrease the excess in negative charge inside the cell. Indeed, it was shown that lowering $[Na^+]_{bl}$ depolarized the basolateral membrane potential in a variety of tissues and that this depolarization resulted from activation of the Na^+-HCO_3^- cotransporter (Boron and Boulpaep, 1983; Yoshitomi et al., 1985; Lopes et al., 1987). We also found that the current was blocked by 4,4′-diisithiocyano-2,2′-stilbene disulfonic acid (DIDS) (*not shown*), a stilbene derivative that binds covalently to the cotransporter anion site (Grassl & Aronson, 1986; Aronson, 1989), and by DNDS, another stilbene derivative that binds in a noncovalent fashion to the Na^+-HCO_3^- cotransporter (Boron & Knakal, 1989) (Figs. 3, 4, 5). As can be seen in Fig. 3, the initial large and rapid increase in I_{sc} observed immediately after reducing $[Na^+]_{bl}$ is followed by a small (2 μA/cm^2) and slow decrease. It is possible that this decrease results from a decrease in the paracellular permeability to Na^+ due to cell swelling caused by permeabilization of cells with amphotericin B. Alternatively, it can be explained by an unstirred layer effect in the lateral intercellular space. Electron microscopy of the monolayers reveal that cells grow tall on porous support and have many convoluted intercellular lateral membrane foldings (Woost et al., 1996). This space is inaccessible to stirring and therefore ion gradients would change with a different time course than in the bulk solutions (Harris et al., 1994).

In the presence of Cl^-, we observed a larger DNDS-sensitive current and conductance components than in its absence. For example DNDS-sensitive current was 1.8-fold and the conductance 2.5-fold greater in the presence of Cl^- than in its absence. This may be explained by the development of a DNDS-sensitive Cl^- conductance which is related to volume regulation. DNDS was shown to inhibit Cl^- conductance in a variety of cells (Cabantchick & Greger, 1992). Variations between cells at different passage numbers provide an additional explanation. Indeed, even in the absence of Cl^-, the DNDS-sensitive conductance varied between 0.12 and 0.22 mS/cm^2 (*see* Table 3 and Fig. 6).

The model presented in Fig. 1 predicts that flux through the cotransporter can be achieved by a $[HCO_3^-]$ gradient. Indeed, we found that lowering $[HCO_3^-]_{bl}$ resulted in generation of a negative current (Fig. 5), consistent with activation of flux through the cotransporter. This current was sensitive to DNDS added to the basal solution, also supporting the involvement of a Na^+-HCO_3^- cotransporter in the basolateral membrane. In intact cells, the exit of negative charge, in response to lowering $[HCO_3^-]_{bl}$, would depolarize the membrane potential. Such a depolarization was observed with a variety of cells (Boron & Boulpaep, 1983; Yoshitomi & Fromter, 1984; Yoshitomi et al., 1985; Lopes et al., 1987; Seki et al., 1993). Alternatively, the effect of lowering $[HCO_3^-]_{bl}$ on I_{sc} could have been accounted for by a simple HCO_3^- conductance (i.e., a channel). However, our observation that reducing $[HCO_3^-]_{bl}$ in the absence of Na^+ had no effect on I_{sc} (*not shown*) argues against a simple HCO_3^- conductance and in favor of a Na^+-HCO_3^- cotransporter. It should be noted that in the experiment described in Fig. 4, the cotransporter was activated by lowering basolateral $[HCO_3^-]$. Since the intracellular ionic composition is mainly determined by the luminal solution, this manipulation should not affect the intracellular concentration of HCO_3^-, which is mainly determined by the luminal solution and the partial pressure of CO_2.

In the second part of this study, we measured the current-voltage relation for permeabilized monolayers and used the DNDS-sensitive current to obtained information about the Na^+-HCO_3^- cotransporter (Fig. 6). Several findings are remarkable: (i) The conductance (the slope of the current-voltage relation) was independent of voltage over a range of 100 mV for both sets of Na^+ concentrations and gradients. There was no evidence for a Goldman-type rectification. (ii) The conductance was essentially the same for both sets of Na^+ concentrations and gradients. These results are consistent with a transporter-mediated process that saturates at the substrate concentrations employed.

In using Eq. 4 to calculate the stoichiometry of HCO_3^- to Na^+ cotransport (*n*) we assumed that the intracellular concentration of HCO_3^- is equal to its extracellular concentration. This is a reasonable assumption, because the concentration of HCO_3^- is determined by pH and CO_2 concentration, both of which equilibrate between the intracellular and luminal compartments. The intracellular pH equilibrates with luminal pH through rapid equilibration of protons across the luminally permeabilized membrane, while CO_2 equilibrates by freely diffusing through the plasma membranes (Yoshitomi & Fromter, 1984).

In conclusion, in this study we found an electrogenic Na^+-HCO_3^- cotransporter in the basolateral membrane of a proximal tubule cell line. The cotransporter exhibited a cotransport stoichiometry of 3 HCO_3^- (or their equivalents, i.e., one HCO_3^- and one CO_3^{2-}) per each Na^+ transported out of the cell. This value is the same as that reported for the cotransporter measured in vivo in

anesthetized rats (Yoshitomi & Fromter, 1985; Yoshitomi et al., 1985); *Necturus* (Lopes et al., 1987) and retinal glial cells (Newman & Astion, 1991); but differs from the 2:1 stoichiometry reported for the cotransporter of rabbit renal cortex (Soleimani et al., 1987), amphibian astrocytes (Astion et al., 1989), amphibian retinal pigment epithelium cells (Hughes et al., 1989), and leech glial cells (Deitmer & Schlue, 1989). The different stoichiometries may reflect differences in species or tissue or perhaps the fact that less direct methods were used in prior studies.

Supported by National Institutes of Health grants HL50173, HL41618 and DK07470-13

References

Akiba, T., Alpern, R.J., Eveloff, J., Calamina, J., Warnock, D.G. 1986. Electrogenic sodium/bicarbonate cotransport in rabbit renal cortical basolateral membrane vesicles. *J. Clin. Invest.* **78:**1472–1478

Alpern, R.J. 1985. Mechanism of basolateral membrane $H^+/OH^-/HCO_3^-$ transport in the rat proximal convoluted tubule. A sodium-coupled electrogenic process. *J. Gen. Physiol.* **86:**613–636

Alpern, R.J., Chambers, M. 1986. Cell pH in the rat proximal convoluted tubule. Regulation by luminal and peritubular pH and sodium concentration. *J. Clin. Invest.* **78:**502–510

Aronson, P.S. 1989. The renal proximal tubule: A model for diversity of anion exchangers and stilbene-sensitive anion transporters. *Ann. Rev. Physiol.* **51:**419–441

Astion, M.L., Chvatal, A., Coles, J.A., Orkand, R.K. 1989. Intracellular pH regulation in glial cells of Necturus optic nerve. *Acta Physiol. Scand.* **136:**64

Biagi, B.A. 1985. Effect of the anion transport inhibitor, SITS, on the proximal straight tubule of the rabbit perfused in vitro. *J. Membrane Biol.* **88:**25–31

Biagi, B.A., Sohtell, M. 1986. Electrophysiology of basolateral transport in the rabbit proximal tubule. *Am. J. Physiol.* **250:**F267–F272

Boron, W.F., Boulpaep, E.L. 1983. Intracellular pH regulation in the renal proximal tubule of the salamander: basolateral HCO_3^- transport. *J. Gen. Physiol.* **81:**53–94

Boron, W.F., Knakal, R.C. 1989. Intracellular pH-regulating mechanism of the squid axon. Interaction between DNDS and extracellular Na^+ and HCO_3^-. *J. Gen. Physiol.* **93:**123–150

Boyarsky, G., Ganz, M.B., Strezel, B., Boron, W.F. 1988. pH regulation in single glomerular mesangial cells. *Am. J. Physiol.* **255:** C857–C869

Burckhardt, B.C., Sato, K., Frömter, E. 1984. Electrophysiological analysis of bicarbonate permeation across the peritubular cell membrane of rat kidney proximal tubule. I. Basic observation. *Pfluegers Arch.* **401:**34–42

Cabantchick, Z.I., Greger, R. 1992. Chemical probes for anion transporters of mammalian cell membranes. *Am. J. Physiol.* **262:**C803–C827

Deitmer, J.W., Schlue, W.R. 1989. An inwardly directed electrogenic sodium-bicarbonate cotransport in leech glial cells. *J. Physiol.* **411:**179–194

Eaton, D.C., Hamilton, K.L., Johnson, K.E. 1984. Intracellular acidosis blocks the basolateral Na^+,K^+ pump in rabbit urinary bladder. *Am. J. Physiol.* **247:**F946–F954

Grassl, S.M., Aronson, P.S. 1986. Na^+/HCO_3^- cotransport in basolateral membrane vesicles isolated from rabbit renal cortex. *J. Biol. Chem.* **261:**8778–8783

Harris, P.J., Chatton, J.Y., Tran, P.H., Bungay, P.M., Spring, K.R. 1994. pH, morphology, and diffusion in lateral intercellular spaces of epithelial cell monolayers. *Am. J. Physiol.* **266:**C73–C80

Hughes, B.A., Adorante, J.S., Miller, S.S., Lin, H. 1989. Luminal electrogenic Na^+HCO_3 cotransport. A mechanism for HCO_3^- absorption across the retinal pigment epithelium. *J. Gen. Physiol.* **94:**125–150

Jentsch, T.J., Keller, S.K., Koch, M., Wiederholt, M. 1984. Evidence for coupled transport of bicarbonate and sodium in cultured bovine corneal endothelial cells. *J. Membrane Biol.* **81:**189–204

Jentsch, T.J., Schill, B.S., Schwartz, P., Matthes, M., Keller, S.K. Wiederholt, M. 1985. Kidney epithelial cells of monkey origin (BSC-1) express a sodium bicarbonate cotransport. *J. Biol. Chem.* **260:**15554–15560

Jentsch, T.J., Schwartz, P., Schill, B.S., Langner, B., Lepple, A.P., Keller, S.K., Wiederholt, M. 1986. Kinetic properties of the sodium bicarbonate (carbonate) symport in monkey kidney epithelial cells (BSC-1). *J. Biol. Chem.* **261:**10673–10679

Kirk, K.L., Dawson, D.C. 1983. Basolateral potassium channel in turtle colon: Evidence for single file flow. *J. Gen. Physiol.* **82:**297–313

L'Allemain, G., Paris, S., Pouyssegur, J. 1985. Role of Na-dependent Cl/HCO_3 exchange in regulation of intracellular pH in fibroblasts. *J. Biol. Chem.* **260:**4877–4883

Lopes, A.G., Siebens, A.W., Giebisch, G., Boron, W.F. 1987. Electrogenic Na^+/HCO_3^- cotransport across basolateral membrane of isolated perfused *Necturus* proximal tubule. *Am. J. Physiol.* **253:** F340–F350

Newman, E.A., Astion, M.L. 1991. Localization and stoichiometry of electrogenic sodium bicarbonate cotransport in retinal glial cells. *Glia* **4:**424–428

Rothenberg, P., Glaser, L., Schlesinger, P., Cassel, D. 1983. Activation of Na/H exchange by epidermal growth factor elevates intracellular pH in A431 cells. *J. Biol. Chem.* **250:**12644–12653

Sasaki, S., Shiigai, T., Takeuchi, J. 1985. Intracellular pH in the isolated perfused rabbit proximal straight tubule. *Am. J. Physiol.* **249:**F417–F423

Seki, G., Coppola, S., Frömter, E. 1993. The Na^+/HCO_3^- cotransporter operates with a coupling ratio of 2 HCO_3^- to 1 Na^+ in isolated rabbit renal proximal tubule. *Pfluegers Arch.* **425:**409–416

Soleimani, M., Grassl, S.M., Aronson, P.S. 1987. Stoichiometry of Na^+-HCO_3^- cotransport in basolateral membrane vesicles isolated from rabbit renalcortex. *J. Clin. Invest.* **79:**1276–1280

Woost, P.G., Orosz, D.E., Jin, W., Frisa, P.S., Jacobberger, J.W., Douglas, J.G., U. Hopfer. 1996. Immortalization and characterization of proximal tubule cells derived from kidneys of spontaneously hypertensive (SHR) and normotensive (WKY) rats. *Kidney Int.* (*in press*)

Yoshitomi, K., Frömter, E. 1984. Cell pH of rat renal proximal tubule in vivo and the conductive nature of peritubular HCO_3^- exit. *Pfluegers Arch.* **402:**300–305

Yoshitomi, K., Frömter, E. 1985. How big is the electrochemical potential difference of Na^+ across rat renal proximal tubular cell membranes in vivo? *Pfluegers Arch.* **405:**S121–S126

Yoshitomi, K., Burckhardt, B.C., Frömter, E. 1985. Rheogenic sodium-bicarbonate cotransport in the peritubular cell membrane of rat renal proximal tubule. *Pfluegers Arch.* **405:**360–366